

## Shift in elastic phase boundaries due to nanoscale phase separation in network glasses: the case of $\text{Ge}_x\text{As}_x\text{S}_{1-2x}$

TAO QU and P. BOOLCHAND\*

Department of Electrical Computer Engineering and Computer Science,  
University of Cincinnati, Cincinnati, OH 45221-0030, USA

(Received 3 August 2004; in final form 3 September 2004)

Binary and ternary sulphide glasses, in contrast to their selenium counterparts, are usually not fully polymerized. This circumstance provides a means to examine the role of nanoscale phase separation effects on global elastic phase diagrams of disordered networks. In bulk  $\text{Ge}_x\text{As}_x\text{S}_{1-2x}$  glasses, the non-reversing enthalpy ( $\Delta H_{\text{nr}}$ ) near  $T_g$  is found to display a global minimum ( $\sim 0$ ) in the  $0.11 < x < 0.15$  range, the *reversibility window*. Furthermore, the  $\Delta H_{\text{nr}}$  term is found to age for glass compositions below ( $x < 0.11$ ) and above ( $x > 0.15$ ) the window, but *not* in the window. In analogy to corresponding selenides, glass compositions in the window represent the *intermediate phase*, those at  $x < 0.11$  are *floppy*, and those at  $x > 0.15$  *stressed-rigid*. Raman scattering shows *floppy* and *stressed-rigid* networks to consist of  $\text{S}_8$ , and  $\text{As}_4\text{S}_4$  and  $\text{As}_4\text{S}_3$  monomers, respectively, aspects of structure that contribute to a narrowing of the intermediate phase and to suppression of the  $\Delta H_{\text{nr}}$  term in S-rich glasses qualitatively in relation to corresponding Se-rich glasses that are fully polymerized.

### 1. Introduction

Lagrangian constraints in mechanics have their origin in the pioneering contribution of Lagrange [1]. Almost a century later, Maxwell [2] applied these ideas to determine the mechanical stability of structures composed of struts and cross-links such as buildings and bridges. And almost a century thereafter, Phillips [3] used these ideas to understand the mechanical behaviour of disordered molecular networks, and enunciated a general principle to account for their glass forming tendency [3, 4]. Thorpe [5] analysed the vibrational behaviour of such molecular networks and recognized that they would spontaneously become *rigid* when the cross-link density or mean coordination number,  $r$ , exceeds a threshold value of 2.40. Recent Raman scattering results [6–9] (see also Chakravarty *et al.*, unpublished) on select selenide glasses, along with numerical simulations [10] and combinatorial calculations [11] have shown that there are in fact *two* elastic phase transitions in disordered networks as a function of increasing  $r$ : a rigidity transition ( $r_c(1)$ ) and a stress transition ( $r_c(2)$ ). In the intervening region,  $r_c(1) < r < r_c(2)$ , a backbone is viewed

---

\* Corresponding author. Email: pboolcha@mail.eecs.uc.edu

to comprise of *select local structures* that are rigid but stress-free. A count of Lagrangian constraints (due to bond-stretching and bond-bending constraints) shows that these local structures possess three constraints per atom ( $n_c$ ), equal to the three degrees of freedom an atom has in a 3d structure. The match insures the stress-free character (isostatically rigid) of the backbone. Networks possessing [10–13]  $r < r_c(1)$  are viewed to be *floppy* (underconstrained,  $n_c < 3$ ), those in the intervening region ( $r_c(1) < r < r_c(2)$ ) to be *intermediate* (optimally constrained,  $n_c = 3$ ) or self-organized, and those at  $r > r_c(2)$  to be *stressed-rigid* (overconstrained,  $n_c > 3$ ).

Calorimetric results on selenide glasses have independently provided thermal fingerprints [7–9, 12–17] (see also Chakravarty *et al.* unpublished) of the three elastic phases, viz. *floppy*, *intermediate* and *stressed-rigid*. Specifically, the *non-reversing enthalpy* ( $\Delta H_{nr}$ ) near  $T_g$  deduced from T-modulated DSC measurements (MDSC) is found to nearly vanish (*thermally reversing windows*) in *intermediate phases*, and to increase by an order of magnitude in both the *floppy* and *stressed-rigid* phases. Glass transitions in *intermediate phases* are thus found to be almost completely *thermally reversing* in character, and furthermore are found not to age. An illustrative example is the case of the  $\text{Ge}_x\text{As}_x\text{Se}_{1-2x}$  ternary [9, 15] on which comprehensive Raman and MDSC results have independently tracked the *rigidity* ( $r_c(1) = 2.27$ ) and *stress* ( $r_c(2) = 2.55$ ) transitions. Both probes independently show [9] the *intermediate phase* to extend over the  $0.09 < x < 0.155$ , or  $2.27 < r < 2.46$  composition range, since  $r = 2 + 3x$  [15].

Numerical simulations [3, 5, 10, 11] of connectivity-related phase transitions in disordered networks generally assume networks to be fully polymerized. On the other hand, in experiments on glasses that condition is not met in general. In this respect the exceptionally simple behaviour of the  $\text{Ge}_x\text{As}_x\text{Se}_{1-2x}$  ternary was discussed in a review [18]. Often, one encounters glass systems that are demixed or segregated on a nanoscale, i.e. composed of covalently bonded backbones interspersed with monomeric species that are decoupled from the backbone. Such monomeric species do not contribute to the connectivity of the backbone and have to be excluded in the count of Lagrangian constraints, thus altering the elastic phase boundaries. Currently, little is known on how elastic phase diagrams would evolve in systems that are intrinsically nanoscale phase separated (NSPS).

Elemental S melts, in contrast to Se ones, do not form bulk glasses upon cooling but instead crystallize into molecular crystals composed of  $\text{S}_8$  crowns. Alloy glasses of S with group IV and V additives at low alloying concentrations, usually consist of weakly polymerized backbones with significant concentrations of  $\text{S}_8$  monomers that are decoupled from the backbones. Ternary  $\text{Ge}_x\text{As}_x\text{S}_{1-2x}$  glasses, for example, in sharp contrast to their selenide counterparts, apparently NSPS not only in the S-rich ( $x < 0.10$ ) but also in the S-deficient ( $x > 2/11$ ) regime, with the former consisting, in part, of  $\text{S}_8$  crowns, while the latter consist of  $\text{As}_4\text{S}_4$  and  $\text{As}_4\text{S}_3$  monomers. Given that the elastic phases in the  $\text{Ge}_x\text{As}_x\text{Se}_{1-2x}$  ternary are well documented [9] and that there exists a commonality of backbone structure between these selenides and their sulphide counterparts, the latter system provides an excellent opportunity to probe the role of NSPS effects on shifting the elastic phase boundaries.

In the present work we have examined ternary  $\text{Ge}_x\text{As}_x\text{S}_{1-2x}$  sulphide glasses over a wide  $0.05 < x < 0.28$  range of compositions in Raman scattering and MDSC experiments. We find the *intermediate phase* to be narrower ( $2.33 < r < 2.45$ ), and backbone-related *ageing effects* outside this *window* to be less pronounced in relation

to those seen in  $\text{Ge}_x\text{As}_x\text{Se}_{1-2x}$  glasses. These results are a direct consequence of NSPS of monomers from the backbone both in S-rich ( $x < 0.08$ ) and S-deficient ( $x > 0.18$ ) compositions. The experimental results are presented in section 2. These results are discussed in section 3, wherein we comment on the nature and extent of the intermediate phase in the present sulphide glasses in relation to corresponding selenide glasses. The conclusions of the present work are summarized in section 4.

## 2. Experimental

Elemental S,  $\text{As}_2\text{S}_3$ , Ge and As of 99.999% purity, from Cerac Inc., were used as starting materials. They were reacted in evacuated quartz ampoules of 5 mm id, homogenized at  $900^\circ\text{C}$  for 48 h and equilibrated at  $50^\circ\text{C}$  above the liquidus before a water quench [9, 15]. Samples were allowed to relax at room temperature for 4 weeks or longer before initiating Raman and MDSC measurements. Raman scattering was excited using 647 nm radiation and the backscattered light collected at  $1\text{ cm}^{-1}$  resolution in a triple monochromator system (Jobin Yvon T 64000) with a CCD detector. The MDSC measurements used a TA Instruments model 2920 unit operated at  $3^\circ\text{C}/\text{min}$  scan rate and  $1^\circ\text{C}/100\text{ s}$  modulation rate.

In figure 1 we compare the MDSC scan of a S-rich glass with that of pure S. Common to both scans is the S polymerization transition (endotherm  $\Delta H_{\text{nr}}(T_\lambda)$ ) near  $T_\lambda = 154^\circ\text{C}$  which constitutes the signature for opening of  $\text{S}_8$  crowns into  $\text{S}_n$  chains [19]. The shape of the non-reversing heat flow associated with the  $T_\lambda$  transition is rather curious; it has a *precursive exothermic* event in the glass but not in pure S. This suggests that  $\text{S}_8$  crowns relax towards the *network backbone* prior to opening into  $\text{S}_n$  chains and being incorporated into the backbone at  $T > T_\lambda$ . The endotherm near  $T = 72^\circ\text{C}$  represents the glass transition, and  $T_g$  was deduced from the inflexion point of the *reversing heat flow* signal [14–18]. The *non-reversing* heat flow associated with  $T_g$  is the hash-marked peak labelled  $\Delta H_{\text{nr}}(T_g)$ . Figure 2 provides a summary of the MDSC results; figure 2(a) shows  $T_g(x)$  to increase with  $x$  except for a glitch near  $x = 0.17$ , figure 2(b) shows variations in  $\Delta H_{\text{nr}}(x)$  displaying a global minimum in the  $0.11 < x < 0.15$  range, and figure 2(c) shows variations in the specific heat jump  $\Delta C_p(x)$  displaying profound ageing effects. Note that within the *thermally reversing window*, the  $\Delta H_{\text{nr}}$  term does not age, although rather striking ageing effects occur for glass compositions outside this *window*.

Figure 3(a) shows the Raman line shapes observed in the glasses as a function of composition  $x$ . Vibrational bands in the  $300\text{--}400\text{ cm}^{-1}$  bond-stretching range result from the Ge- and As-centred local structures that contribute to the network backbone as discussed previously [9, 20]. Figure 3(b) shows an enlarged view of the sharp modes (boxed area) observed in the spectrum of a glass at  $x = 0.20$ . This glass composition corresponds to  $y = 1/2$  in the  $(\text{As}_2\text{S}_3)_y(\text{Ge}_2\text{S}_3)_{1-y}$  ternary that was recently investigated in Raman scattering and MDSC measurements by Mamedov *et al.* [20]. The octet of modes labelled  $\nu_n$ , with  $n$  going from 1 to 8, reported here are in harmony with the results of Mamedov *et al.* [20]. Molar volumes ( $V_m$ ) of the glasses were recently reported by Aitken and Ponader [21] and their results are reproduced for the reader's convenience in figure 3(c). In figure 3(c), we also compare variations in  $V_m$  with those in Raman mode ( $\nu_6$  and  $\nu_8$ ) scattering strengths as a function of  $x$ , and note that all these observables show a global maximum near the glass composition,  $x = 0.20$ .

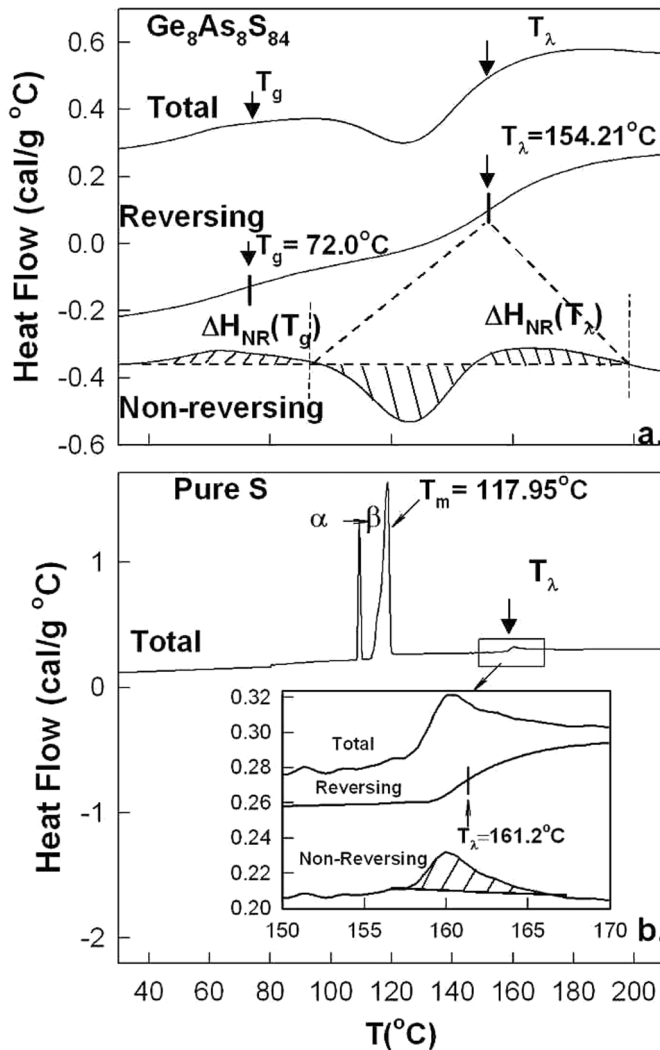


Figure 1. MDSC scan of (a)  $x=0.08$  sulphide glass and (b) pure S taken at  $3^\circ\text{C}/\text{min}$  and  $1^\circ\text{C}/100\text{s}$  modulation rate. Common to both scans is the sulphur polymerization transition  $T_\lambda$  near  $159^\circ\text{C}$ . Note that the non-reversing heat associated with the  $T_\lambda$  transition has a precursive exotherm in the glass but not in pure S (inset of (b)). In pure S, we observe the  $\alpha \rightarrow \beta$  transition near  $102^\circ\text{C}$  and the melting transition near  $118^\circ\text{C}$ .

### 3. Discussion

#### 3.1. Molecular structure of $\text{Ge}_x\text{As}_x\text{S}_{1-2x}$ glasses

The Raman scattering results of figure 3 provide an overview of glass molecular structure evolution with cation concentration  $x$ . At low  $x$  ( $<0.10$ ) the structure is dominated by  $\text{S}_8$  crowns and  $\text{S}_n$  chain fragments, both of which contribute to the sharp modes observed near  $150\text{cm}^{-1}$ ,  $217\text{cm}^{-1}$  and  $485\text{cm}^{-1}$ . And as we discuss in section 3.2, it is possible to separate the contributions of  $\text{S}_8$  crowns from  $\text{S}_n$  chain segments in MDSC measurements largely because the former conformation

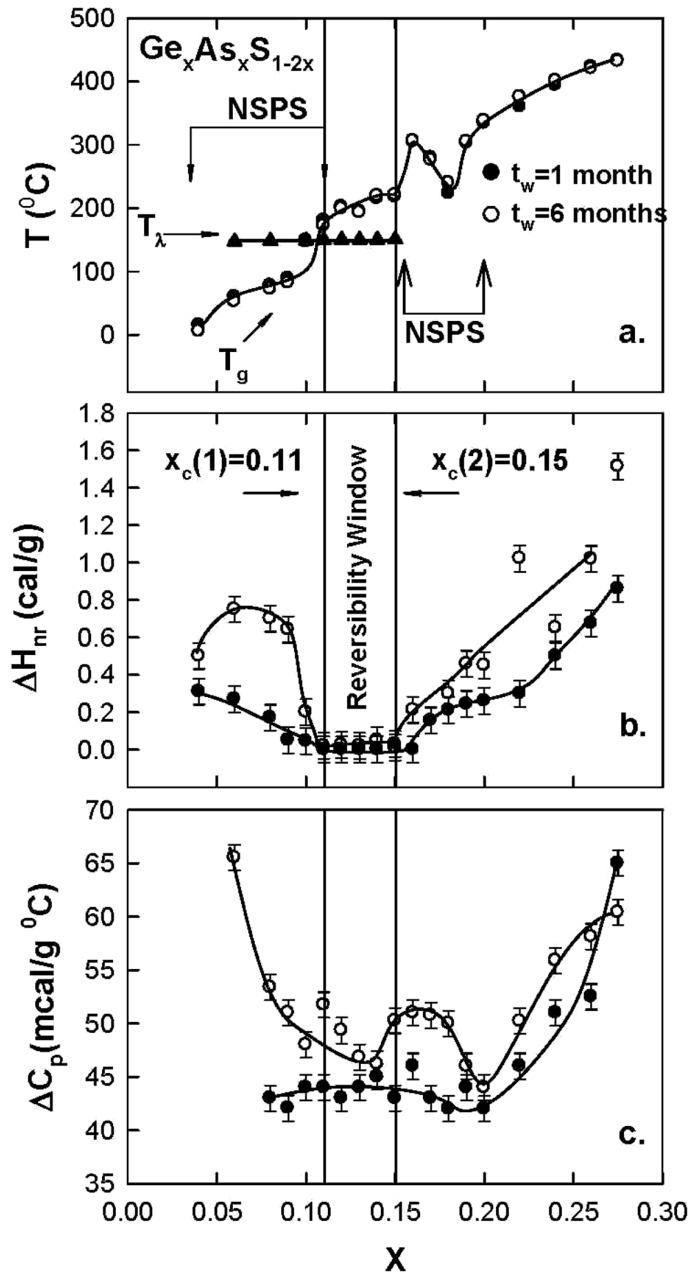


Figure 2. Summary of MDSC results for sulphide glasses showing trends in (a) the glass transition temperature,  $T_g(x)$ , (b) the non-reversing heat,  $\Delta H_{nr}(x)$  and (c) the specific heat jump near  $T_g$ ,  $\Delta C_p(x)$ , as a function of glass composition. Note the reversibility window in the  $0.11 < x < 0.15$  range in (b).

contributes to the  $T_\lambda$  transition while the latter contributes to the  $T_g$  transition. The scattering in the  $300\text{ cm}^{-1}$  to  $400\text{ cm}^{-1}$  range comes from both As-centred and Ge-centred cross-links of  $S_n$  chain fragments that nucleate the backbone in these ternary glasses. With increasing  $x$ , the scattering in the  $300\text{ cm}^{-1}$  to  $400\text{ cm}^{-1}$  range

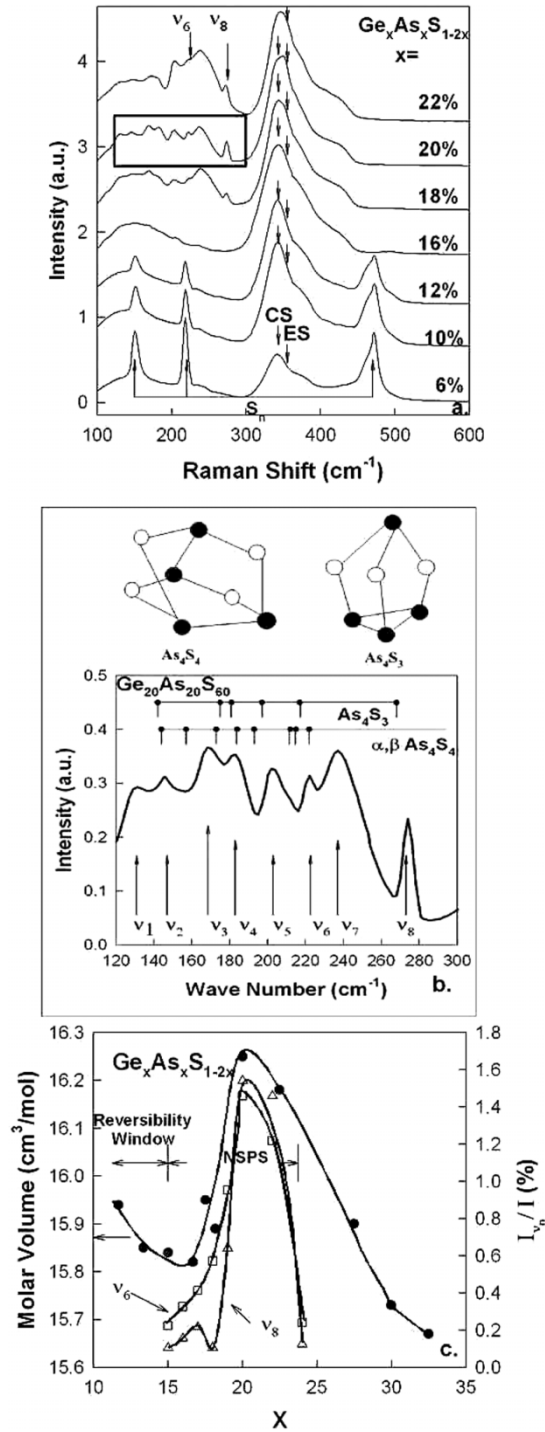


Figure 3. (a) Raman scattering in sulphide glasses as a function of increasing  $x$ . (b) Enlarged view of sharp modes observed in the  $150\text{--}300\text{ cm}^{-1}$  range; boxed area, for a sample at  $x = 0.20$ . (c) Molar volumes of the glasses taken from [21] and scattering strength of Raman modes  $v_6$  and  $v_8$  from the present work showing a maximum near  $x = 0.20$ , ascribed to partial NSPS.

increases sharply at the expense of the sharp S modes with  $x$  underscoring a precipitous growth of the network backbone in the  $0.10 < x < 0.18$  range. In this range of chemical composition the principal building blocks of the backbone consist of As-centred quasi-tetrahedral (QT),  $\text{AsS}(\text{S}_{1/2})_3$  and pyramidal (PYR),  $\text{As}(\text{S}_{1/2})_3$  units, and Ge-centred corner-sharing (CS)  $\text{GeS}_4$ , and edge-sharing (ES)  $\text{GeS}_2$  units.

In the present ternary, a chemical threshold ( $x = x_t$ ) is predicted [9] to occur when all sulphur becomes bonded in As-centred and Ge-centred local structures,

$$\text{As}_x\text{Ge}_x\text{S}_{1-2x} = (5x/2)(\text{As}_{2/5}\text{S}_{3/5}) + 3x(\text{Ge}_{1/3}\text{S}_{2/3}) + \text{S}_{1-11x/2} \quad (1)$$

leaving the coefficient of the free S term in equation (1) to vanish at the threshold,  $x = x_t$ , i.e.  $1 - 11x_t/2 = 0$ , or  $x_t = 2/11$  or 0.182. At  $x > x_t$ , one expects homopolar (As–As, Ge–Ge) bonds to manifest in the network. In the present ternary, As–As bonds apparently first manifest in  $\text{As}_4\text{S}_4$  and  $\text{As}_4\text{S}_3$  monomers in the  $0.16 < x < 0.23$  range as revealed by Raman scattering. Of the octet of modes observed at  $x = 0.20$  (figure 3(b)),  $\nu_6$  and  $\nu_8$  come exclusively from  $\text{As}_4\text{S}_4$  and  $\text{As}_4\text{S}_3$  monomers [20], respectively. And the correlation in scattering strengths of these modes with molar volumes (figure 3(c)) showing a global maximum near  $x = 0.20$ , serves to confirm [20] that glasses in the  $0.16 < x < 0.23$  range are partially NSPS. The non-bonding van der Waals forces segregate these monomers from each other and the backbone. Here we must remember that the sulphur van der Waals radius [22] (180 pm) is nearly twice as large as the sulphur covalent radius (102 pm). NSPS leads to a loss in network packing that is reflected in the molar volumes acquiring a maximum near  $x = 0.20$ . The result is in harmony with the Raman scattering strength of the  $\nu_6$  and  $\nu_8$  modes, that peak near  $x = 0.20$ . These modes were identified [20] with the two monomers in question,  $\text{As}_4\text{S}_4$  and  $\text{As}_4\text{S}_3$  (figure 3(b)).

### 3.2. The intermediate phase of $\text{Ge}_x\text{As}_x\text{S}_{1-2x}$ glasses

In figure 4, we compare the *thermally reversing window* in ternary  $\text{Ge}_x\text{As}_x\text{Se}_{1-2x}$  glasses [9, 15] ( $2.27 < r < 2.46$ ) with that observed in the present glasses ( $0.11 < x < 0.15$ , or  $2.33 < r < 2.45$  range). By analogy, we identify the latter window as the *intermediate phase* of the present glasses. The nature of the isostatic building blocks in the two ternaries share commonality, and consist of As-centred quasi-tetrahedral (QT),  $\text{AsX}(\text{X}_{1/2})_3$  and pyramidal (PYR)  $\text{As}(\text{X}_{1/2})_3$  units, and Ge-centred corner-sharing (CS)  $\text{GeX}_4$ , and edge-sharing (ES)  $\text{GeX}_2$  units with  $\text{X} = \text{S}$  or  $\text{Se}$ . For each of these units,  $n_c = 3$ , as reported previously [15]. The mean coordination number,  $r$ , of the QT, PYR, CS and ES units, respectively, is 2.27, 2.40, 2.40 and 2.67 and the intrinsic spread of  $r$  of these units serves to determine the width of the *intermediate phase*.

The lower edge of the intermediate phase at  $r_c(1) = 2.33(1)$  in the present sulphides (figure 4) is upshifted in relation to that in selenides ( $r_c(1) = 2.27(1)$ ), presumably because a significant amount of S segregates into the  $\text{S}_8$  crowns in S-rich glasses and thereby inhibits growth of the backbone. This view is corroborated by the sharp reduction in  $T_g$  at  $x < 0.10$  as  $\text{S}_8$  crowns segregate from the backbone. In our MDSC scans the fraction of the non-reversing enthalpy associated with the  $T_\lambda$  transition, i.e.  $\Delta H_{\text{nr}}(T_\lambda)/[\Delta H_{\text{nr}}(T_\lambda) + \Delta H_{\text{nr}}(T_g)]$ , is found to systematically decrease by a factor of 3.2(1) as  $x$  increases from 0.08 to 0.11. This fraction is a good representation of the  $\text{S}_8$  fraction in the glasses, and its reduction with increasing  $x$

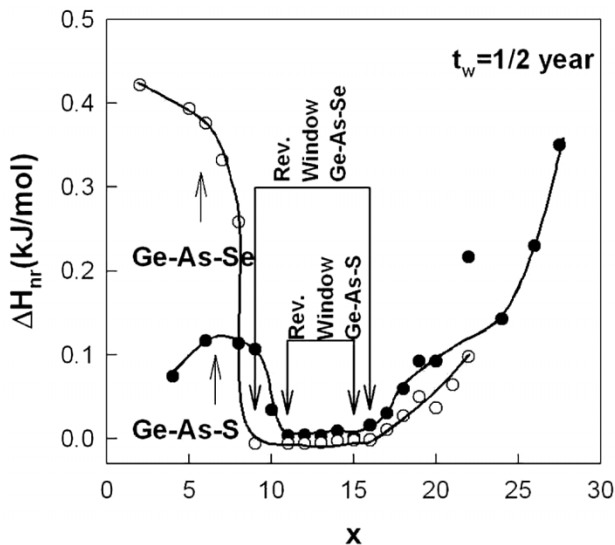


Figure 4. (a) Molar non-reversing enthalpy,  $\Delta H_{nr}(x)$ , in  $\text{Ge}_x\text{As}_x\text{S}_{1-2x}$  glasses ( $\bullet$ ) and  $\text{Ge}_x\text{As}_x\text{Se}_{1-2x}$  glasses ( $\circ$ ) taken after 6 months' waiting time ( $t_w$ ). Note the smaller width of the reversibility window in the sulphides than for the selenides. Also note the much smaller enthalpy in S-rich glasses than in the Se-rich glasses because of qualitative loss of the backbone due to NSPS in the former as  $x \rightarrow 0$ .

highlights growth of the backbone in which rigidity can percolate. Furthermore, in Raman scattering we find the normalized scattering strength of the sharp modes near  $150$ ,  $218$  and  $470\text{ cm}^{-1}$  that have contributions due to both sulphur chains and rings systematically decrease by a factor of  $1.9(1)$  as  $x$  increases from  $x = 0.08$  to  $0.11$ . In Raman scattering, separation of rings from chains is less trivial, nevertheless the trend is similar. The upper edge of the intermediate phase is at  $r_c(2) = 2.45$ , nearly the same as in the case of the selenides,  $r_c(2) = 2.46$ . Not surprisingly, the  $\text{S}_8$  concentration extrapolates to zero near  $r \sim 2.40$ . Interestingly, a small but decreasing concentration of  $\text{S}_8$  crowns persists in the *intermediate phase* of the present glasses, and apparently that does not influence the *self-organized* nature of the backbone, probably because  $\Delta H_{nr}$  is intrinsically a backbone property. This result broadly supports the *robust* nature of the intermediate phase in these ternary glasses.

### 3.3. Ageing of network glasses

The non-reversing enthalpy near  $T_g$ ,  $\Delta H_{nr}$ , in general, is found to age in network glasses as a function of waiting time. There are recent results to show that the ageing function of the  $\Delta H_{nr}$  term is a stretched exponential. Furthermore, in a region of optimal coordination ( $r = 2.4$ ), network glasses are found to behave differently, in that their ageing is qualitatively suppressed [16, 23]. Here it is important to recognize that lack of ageing can also result trivially from the absence of a network backbone in a glass, as revealed by the present results on sulphide glasses.

We have compared in figure 4 ageing of the  $\Delta H_{nr}$  term in the present sulphide glasses with that in corresponding selenides, particularly in the floppy regime. Both sets of MDSC measurements were performed 6 months after melt-quenching, with



glass samples aged at room temperature below  $T_g$ . For both sets of glasses,  $T_g$  values are about the same in the floppy regime. We note that  $\Delta H_{nr} \sim 0.40$  kJ/mol in selenide glasses at  $x=0.06$ , but only 0.10 kJ/mol for the corresponding sulphide glasses. The four-fold reduction of  $\Delta H_{nr}$  reflects the loss of backbone in the sulphide glasses in relation to the selenide glasses. Thus, the upshift of the rigidity transition ( $x_c(1)$ ) to higher  $x$ , and the remarkable *loss in ageing* of the  $\Delta H_{nr}$  term in the present sulphide glasses reflects a backbone structure that is not as well developed as in their selenide counterparts, because of the presence of a significant concentration of decoupled  $S_8$  monomers in the floppy phase.

The absence of ageing of the backbone in the intermediate phase of the present ternary sulphide glasses is strikingly illustrated by our results shown in figure 2(b). We find that the  $\Delta H_{nr}$  term in the  $0.11 < x < 0.15$  range in the 1 month and 6 month aged samples remains minuscule ( $\sim 0$ ). On the other hand, the  $\Delta H_{nr}$  term is found to increase by almost an order of magnitude at  $x < 0.11$  (floppy phase) and at  $x > 0.15$  (stressed-rigid phase). A strikingly similar pattern has been observed in ternary  $Ge_xP_xSe_{1-2x}$  glasses [23]. These results form part of a general pattern showing glass compositions in the intermediate phase to form backbones that are isostatically rigid. Isostaticity also accounts for the non-ageing behaviour of glasses in the intermediate phase.

#### 4. Conclusions

In summary, MDSC measurements on  $As_xGe_xS_{1-2x}$  glasses reveal that the *reversibility window* is in the range  $0.11 < x < 0.15$ . Ageing of the non-reversing enthalpy is observed for glass compositions outside the window, but *not* in the *window*. A distinguishing feature of the present glasses is that  $S_8$  crowns segregate from the backbone qualitatively in the *floppy* regime, as observed by both Raman scattering and MDSC measurements. The qualitative loss of backbone suppresses ageing of the non-reversing enthalpy in S-rich glasses in relation to the corresponding Se-rich glasses.

#### Acknowledgements

We have benefited from discussions with D. McDaniel, B. Goodman and Ping Chen during the course of this work. This work is supported by NSF grant DMR-01-01808.

#### References

- [1] J.L. Lagrange, *Mechanique Analytique* (1788).
- [2] J.C. Maxwell, *Phil. Mag.* **27** 294 (1864).
- [3] J.C. Phillips, *J. non-crystalline Solids* **34** 153 (1979); *ibid.* **43** 37 (1981).
- [4] R. Kerner and J.C. Phillips, *Solid St. Commun.* **117** 47 (2000).
- [5] M.F. Thorpe, *J. non-crystalline Solids* **57** 355 (1983).
- [6] X. Feng, W.J. Bresser and P. Boolchand, *Phys. Rev. Lett.* **78** 4422 (1997).
- [7] D. Selvanathan, W.J. Bresser and P. Boolchand, *Phys. Rev. B* **61** 15061 (2000).
- [8] P. Boolchand, X. Feng and W.J. Bresser, *J. non-crystalline Solids* **293–295** 348 (2001).
- [9] T. Qu, D.G. Georgiev, P. Boolchand, *et al.*, *Mater. Res. Soc. Proc.* **754** 111 (2003).
- [10] M.F. Thorpe, D.J. Jacobs, M.V. Chubynsky, *et al.*, *J. non-crystalline Solids* **266–269** 859 (2000).

- [11] M. Micoulaut and J.C. Phillips, *Phys. Rev. B* **67** 104204 (2000).
- [12] P. Boolchand, D.G. Georgiev and B.J. Goodman, *Optoelectron. Adv. Mater.* **3** 703 (2001).
- [13] J.C. Phillips, *Phys. Rev. Lett.* **88** 216401 (2002).
- [14] D.G. Georgiev, P. Boolchand and M. Micoulaut, *Phys. Rev. B* **62** R9228 (2000).
- [15] Y. Wang, P. Boolchand and M. Micoulaut, *Europhys. Lett.* **52** 633 (2000).
- [16] P. Boolchand, D.G. Georgiev and M. Micoulaut, *J. Optoelect. Adv. Mater.* **4** 823 (2002).
- [17] D.G. Georgiev, P. Boolchand, H. Eckert, *et al.*, *Europhys. Lett.* **62** 49 (2003).
- [18] P. Boolchand, D.G. Georgiev, T. Qu, *et al.*, *Comptes Rendus Chemie* **5** 713 (2002).
- [19] N.N. Greenwood and E. Earnshaw, *Chemistry of Elements* (Pergamon, Oxford, 1984), p. 781. Also see M. Stolz, R. Winter, W.S. Howells, *et al.*, *J. Phys: condensed Matter* **6** 3619 (1994).
- [20] S. Mamedov, D.G. Georgiev, T. Qu, *et al.*, *J. Phys: condensed Matter* **15** S2397 (2003).
- [21] B.G. Aitken and C.W. Ponader, *J. non-crystalline Solids* **256/257** 143 (1999); *ibid.* **274** 124 (2000).
- [22] B. Douglas, D. McDaniel and J. Alexander, *Concepts and Models of Inorganic Chemistry* (Wiley, New York, 1994), p. 101.
- [23] S. Chakravarty, D.S. Georgiev, P. Boolchand, *et al.*, *Cond-Mat/0308016* (2003).